Original Article

Identification of solute carrier family genes related to the prognosis and tumor-infiltrating immune cells of pancreatic ductal adenocarcinoma

Yuhua Meng[1#], Yanting Li[1#], Dalang Fang[2], Yuanlu Huang[1]

[1]Department of Glandular Surgery, the People's Hospital of Baise, Baise, China; [2]Department of Breast and Thyroid Surgery, The Affiliated Hospital of Youjiang Medical University for Nationalities, Baise, China

Contributions: (I) Conception and design: Y Huang, D Fang; (II) Administrative support: Y Huang; (III) Provision of study materials or patients: Y Meng, Y Li; (IV) Collection and assembly of data: Y Meng, Y Li; (V) Data analysis and interpretation: Y Meng, Y Li; (VI) Manuscript writing: All authors; (VII) Final approval of manuscript: All authors.

[#]These authors contributed equally to this work.

Correspondence to: Yuanlu Huang. Department of Glandular Surgery, the People's Hospital of Baise, Baise, China. Email: HYL81259@163.com; Dalang Fang. Department of Breast and Thyroid Surgery, The Affiliated Hospital of Youjiang Medical University for Nationalities, Baise, China. Email: fangdalang@stu.gxmu.edu.cn.

Background: Pancreatic ductal adenocarcinoma (PDAC) has persisted as one of the worst prognostic tumors with a 5-year survival rate of lower than 6%. Although many studies have investigated PDAC, new biomarkers are required to ensure early diagnosis and predict the prognosis of PDAC.

Methods: In this study, we used bioinformatics methods to evaluate differences in the expression of solute carrier (SLC) family genes in tumors and non-tumors. A Kaplan-Meier analysis, least absolute shrinkage and selection operator (LASSO) analysis, and multivariate Cox proportional hazards regression analysis were used to evaluate the relationship between SLC genes and prognosis using The Cancer Genome Atlas (TCGA) and Gene Expression Omnibus (GEO) datasets. The prognostic signature was constructed depending on the risk score to assess the impact of multiple genes on the prognosis, receiver operating characteristic (ROC) curves and forest plot was constructed to assess the ability to predict the prognosis and effects of clinical variables in both high- and low-risk groups. Tumor-infiltrating immune cells were evaluated using Cell-type Identification by Estimating Relative Subsets of RNA Transcripts (CIBERSORT) in both high- and low-risk groups.

Results: In 32 SLC genes, 9 were significantly associated with the OS after LASSO analysis. *SLC19A3* (P=0.007), *SLC25A39* (P=0.027), *SLC39A11* (P=0.043) were significantly associated with prognosis and included into the prognostic model. CIBERSORT demonstrated that memory B cells (P=0.004), naive B cells (P=0.007), CD8 T cells (P=0.003), activated memory CD4 T cells (P=0.004), and activated NK cells (P=0.019) were significantly higher in the low-risk group. Gene set enrichment analysis (GSEA) showed that potential molecular mechanisms enriched in *MYC* and *p53* signaling pathways.

Conclusions: *SLC19A3*, *SLC25A35*, and *SLC39A11* were significantly relative to the prognosis of PDAC and changed the tumor microenvironment, as well as the *MYC* and *p53* signaling pathways. The *SLC19A3* gene may represent a new tumor suppressor in PDAC.

Keywords: Solute carrier genes; prognosis; tumor-infiltrating immune cells; pancreatic ductal adenocarcinoma (PDAC)

Submitted Nov 08, 2021. Accepted for publication Dec 23, 2021.
doi: 10.21037/atm-21-6341
View this article at: https://dx.doi.org/10.21037/atm-21-6341

Introduction

Pancreatic cancer (PC) is the fourth and the sixth leading cause of cancer-related death in the US and China, respectively (1,2). In 2018, there were approximately 458 million new cases and 432 million deaths due to PC (3). The above statistics indicate that PC is a highly malignant neoplasm with a similar morbidity and mortality; and the 5-year survival rate remains low, at 6% (4). Pancreatic ductal adenocarcinoma (PDAC) is the predominant pathological type of PC (5). Patients with PDAC are typically first diagnosed at an advanced stage, and thus, have surpassed the opportunity for surgical treatment. This is because patients do not exhibit classic symptoms at an early stage and there is an absence of powerful detective biomarkers (6). Some patients are lucky and undergo radical resection; however, the 5-year survival rate is only as high as 25% (7). Thus, new biomarkers are required to improve outcomes.

The solute carrier (SLC) gene superfamily is the second largest family of membrane proteins after G protein-coupled receptors, including over 400 proteins in 65 subfamilies based on sequence similarities (8). Amino acids, sugars, fatty acids, inorganic ions, essential metals, and drugs are transported over the cell membrane by the SLCs, which function as passive transporters, ion transporters, and exchangers (9). Since SLCs are responsible for transporting essential substances throughout the human body, SLC mutations have been linked to human genetic disorders and the level of SLC expression is changed in a variety of tumors, including congenital chloride diarrhea, glucose galactose malabsorption, and familial renal glucosuria (10-12). A study showed that *SLC5A8* could suppress colon cancer and was silenced by methylation (13). In a mouse model, reducing polyamine was effective for prolonging prognosis and preventing tumor progression, and a knockdown of *SLC3A2* in neuroblastoma cells reduced the uptake of polyamine (14). Moreover, SLCs have been extensively studied in pharmacokinetics, chemotherapy resistance, and as therapeutic targets (15). Nucleoside transporters encoded by the *SLC28* and *SLC29* subfamilies have been shown to mediate the uptake of gemcitabine and 5-fluorouracil. In addition, some of the *SLC22A* subfamily is related to the transport of platinum compounds (16,17). Mutations of SLC affect the synthesis of transporters, finally resulting in an insufficient intake of chemotherapeutic drugs which will inevitably lead to decreased sensitivity to chemotherapy. Although a previous study found that SLC2A1 may be a prognostic biomarker for PDAC, the SLC family played an important role in biological processes such as metabolism, and the comprehensive analysis of the SLC family in PDAC was still unknown (18). As well as, the potential mechanism of most members of the SLC family in PDAC and the relationship between genes and the prognosis of PDAC remains unclear.

The tumor microenvironment (TME) consists of multiple cell types (e.g., endothelial cells, immune cells, and so on) and extracellular components. Tumor cells can alter the TME through immune escape and immunosuppression; thus, the TME plays a critical role in the occurrence, progression, and treatment of tumors (19,20). In addition, immune cells are an essential cell type involved in TME and targeting immune cells is a promising therapy in PC (21). The effect of PD1 or PD-L1 checkpoint inhibitor immunotherapy has improved the clinical outcomes in a variety of tumors, including advanced melanoma, Hodgkin's lymphoma, and advanced gastric or gastro-esophageal junction cancer (22-24). However, targeting immune checkpoints has not benefited all patients in a variety of tumors, including PDAC (25). Researching the differences in tumor-infiltrating immune cells (TIICs), the relationship with molecular expression and interactive features in individual tumors, and therefore, the identification of new immunotherapeutic targets, is critical for improving patient prognosis. Studies shown that the tumor microenvironment of PDAC was highly heterogeneous, and PD-1+ cells, and Foxp3+ T cells could evaluate the prognosis of patients with PDAC after surgery (26,27). A study shown that SLC1A5, SLC7A5, SLC3A2 were associated with the expression of PD1 and PD-L1, and might be associated with subtypes of immune cell infiltration. Therefore, we speculated that the SLC family could play a role in the TME of PDAC, especially TIICs (28).

In this study, we collected data from The Cancer Genome Atlas (TCGA) and Gene Expression Omnibus (GEO) databases, using bioinformatics tools to explore the relationship between SLC family genes and prognosis of PDAC patients, the underlying molecular mechanisms, and the density of numerous TIICs associated with clinicopathological characteristics. These results are promising for providing a new perspective on the TME and identifying potential biomarkers to achieve better clinical outcomes of PDAC.

We present the following article in accordance with the TRIPOD reporting checklist (available at https://atm.amegroups.com/article/view/10.21037/atm-21-6341/rc).

Methods

Data collection

We downloaded RNA-Seq expression profiles and clinical data from the publicly available TCGA (https://cancergenome.nih.gov/) and the University of California, Santa Cruz Xena (UCSC Xena: https://xena.ucsc.edu/) databases, respectively (29). The raw expression profiles were normalized using *DESeq* package in R (29). The following inclusion criteria were previously published by our research team: (I) complete survival data available; (II) histology type was PDAC; (III) pathologic stage I or II; and (IV) patients underwent pancreaticoduodenectomy. Any PDAC patients with pathologic stage III or IV disease who underwent other types of surgery were excluded (30). To investigate whether there are differences in gene expression in the peripheral blood (PB) and peripheral blood mononuclear cells (PBMCs), GSE49641 and GSE74629 were downloaded from the GEO database. If there were multiple expression values for the same gene name, the average value and expression profiles were normalized using the *limma* package in R (https://bioconductor.org/packages/release/bioc/html/limma.html). The study was conducted in accordance with the Declaration of Helsinki (as revised in 2013).

Survival analysis

A Kaplan-Meier analysis was used to assess prognosis-related clinical factors. Patients were divided into low- and high-expression groups according to the median gene expression value. We used Kaplan-Meier analysis to preliminarily screen for the genes related to prognosis. Next, a least absolute shrinkage and selection operator (LASSO) algorithm was used to select the strongest prognostic-related genes. Prognostic-related genes were finally defined by a Cox proportional risk regression model that was adjusted by prognostic-related clinical factors.

Bioinformatics analysis

The Gene Expression Profiling Interactive Analysis (GEPIA; https://gepia.cancer-pku.cn/index.html) website was used to evaluate differences in gene expression in both the tumor and non-tumor tissues (31). The protein-protein interaction (PPI) network, Gene Ontology (GO), and Kyoto Encyclopedia of Genes and Genomes (KEGG) analysis was obtained from the Search Tool for the Retrieval of Interacting Genes/Proteins (STRING; https://string-db.org/, version 11) (32). The results of the LASSO analysis of SLCs were entered into the website, and further obtained after setting *Homo sapiens* and an interaction score >0.150. The KEGG results were visualized using R. We then used GeneMANIA (https://genemania.org/) to acquire details of gene-gene interactions (33). A Pearson's correlation coefficient between the SLC genes was calculated, and the *corrplot* package in R (https://cran.r-project.org/web/packages/corrplot/index.html) was used to visualize the results. The differences in SLC expression between PDAC and healthy controls in PB and PBMCs were analyzed and plotted using the *ggplot2* package in R (https://cran.r-project.org/web/packages/ggplot2/index.html).

Joint-effect analysis and prognostic signature construction

To increase the applicability of the results, we used the prognostic-related genes to establish a joint-effect analysis with a Kaplan-Meier analysis. Nomograms were constructed using clinical variables and prognostic-related genes were used to predict the overall survival (OS) for PDAC using the *rms* package (https://cran.r-project.org/web/packages/rms/index.html). A prognostic risk model was constructed using prognostic-related genes. SLC19A3, SLC25A39, and SLC39A11 were included in nomogram because only they satisfied prognosis-related genes and differential expression in both the tumor and normal tissues. Regression coefficients were obtained from the results of the multivariate Cox proportional hazards regression analysis. The calculation formula for the risk score was as follows (30):

Risk score = expression of $gene_1 \times \beta_1$ + expression of $gene_2 \times \beta_2$+… expression of $Gene_n \times \beta_n$.

The participants were divided into high- and low-risk groups based on their risk score. Receiver operating characteristic (ROC) curves were constructed to assess the accuracy of the prognostic signature using prognostic-related genes and risk score. A forest plot was constructed to assess whether the risk model was combined with other clinical factors, which has an impact on the prognosis.

CIBERSORT estimation

To investigate the TIIC landscape in the PDAC tissue between the high- and low-risk groups, the Cell-type Identification by Estimating Relative Subsets of RNA Transcripts (CIBERSORT) algorithm (https://cibersort.

stanford.edu) was used to calculate the absolute proportions of 22 types of TIICs (34). CIBERSORT, which contained 547 genes, could accurately differentiate 22 individual immune cell types from the tumor is a deconvolution algorithm and is the most widely used method to date (35). A normalized PDAC dataset was input as a mixture file, 22 immune cell types (LM22) were set as the signature gene file, and an analysis was performed at 1,000 permutations. The samples which resulted in P<0.05 were considered statistically significant. We used the *corrplot* package in R to visualize the Pearson's correlation coefficient between different immune cells. A bar graph was constructed using *barplot* packages to demonstrate a landscape of TIICs for statistically significant cases. The differences in TIICs between high- and low-risk groups were shown in a violin plot.

Gene set enrichment analysis (GSEA)

GSEA is an algorithm that can use known gene expression to calculate the potential mechanisms of differential gene expression, affecting the prognosis of patients (36). High- and low-group files determined by prognostic-related genes and genome-wide expression profile were uploaded to the GSEA. We included C2 and C5 of the Molecular Signatures Database (MSigDB) in the enrichment analysis (37). Meeting both the false discovery rate (FDR) <0.25 and P<0.05 was considered statistically significant evidence (38).

Statistical analysis

The statistical analyses were conducted using SPSS software version 22.0 (IBM Corp., Armonk, NY, USA) and R-project version 3.6.3 (https://cran.r-project.org/bin/windows/base/old/3.6.3/). The Kaplans://cr method was used to calculate the median survival time and log-rank P value. Hazard ratios (HRs) and 95% confidence intervals (CI) were calculated using the univariate and multivariate Cox proportional hazards regression model. A P value <0.05 was considered statistically significant.

Results

Data collection

A total of 183 pancreatic adenocarcinoma (PAAD) cases were downloaded, and after applying the inclusion and exclusion criteria, 112 PDAC cases were finally included in the follow-up research in TCGA. In total, 36 and 50 PDAC and non-tumor patients, respectively, were included from GSE49641 and GSE74629 in the subsequent analyses.

Survival analysis

Prognosis-related clinical variables are shown in Table S1, and the histologic grade, targeted molecular therapy, radiation therapy, and residual resection were shown to significantly affect the patient's prognosis. The results of the prognostic differences from the low- and high-expression groups of each SLC are presented in Table S2. In addition, 32 SLC genes were significantly associated with the OS. The genes *SLC19A3*, *SLC22A23*, *SLC22A4*, *SLC25A11*, *SLC25A39*, *SLC26A10*, *SLC35B4*, *SLC35E2*, *SLC39A11*, *SLC46A2*, *SLC47A1*, and *SLC52A1* were the results of the LASSO analysis (*Figure 1A*,*1B* and Figure S1). After calculation using a Cox proportional risk regression model, *SLC19A3* (adjusted P=0.007), *SLC22A23* (adjusted P=0.035), *SLC25A39* (adjusted P=0.027), *SLC39A11* (adjusted P=0.043), and *SLC47A1* (adjusted P=0.024) were significantly correlated with the prognosis (*Table 1*).

Bioinformatics analysis

The Pearson's correlation coefficient from the 12 genes selected from LASSO analysis are presented in *Figure 1C*. The genes *SLC47A1* and *SLC46A2*, *SLC35B4* and *SLC47A1*, and *SLC46A2* were moderately positive in relation to each other (coefficient >0.5), whereas *SLC35B4* was moderately negative in relation to *SLC25A39* (coefficient <–0.5). The gene-gene interactions displayed in *Figure 2A* show a strong co-expression relationship between these genes. The PPI is presented in *Figure 2B* and shows interactions in expression, experiment, text-mining, and co-expression. The GO and KEGG pathway enrichment analyses were mainly enriched in acids, inorganic ions, and essential metal transmembrane transporter activity (*Figure 2C*). The distribution in SLC expression between PAAD tumor and normal tissues from GEPIA suggested that the expression of *SLC39A11*, *SLC25A39*, *SLC22A4*, *SLC35B4*, *SLC25A11*, and *SLC19A3* were significantly higher in the tumor tissue (*Figure 3*). In PB, the level of *SLC22A4*, *SLC25A11*, and *SLC46A2* expression in PDAC patients was higher than that in the control samples (Figure S2). In PBMCs, only *SLC35E2* exhibited

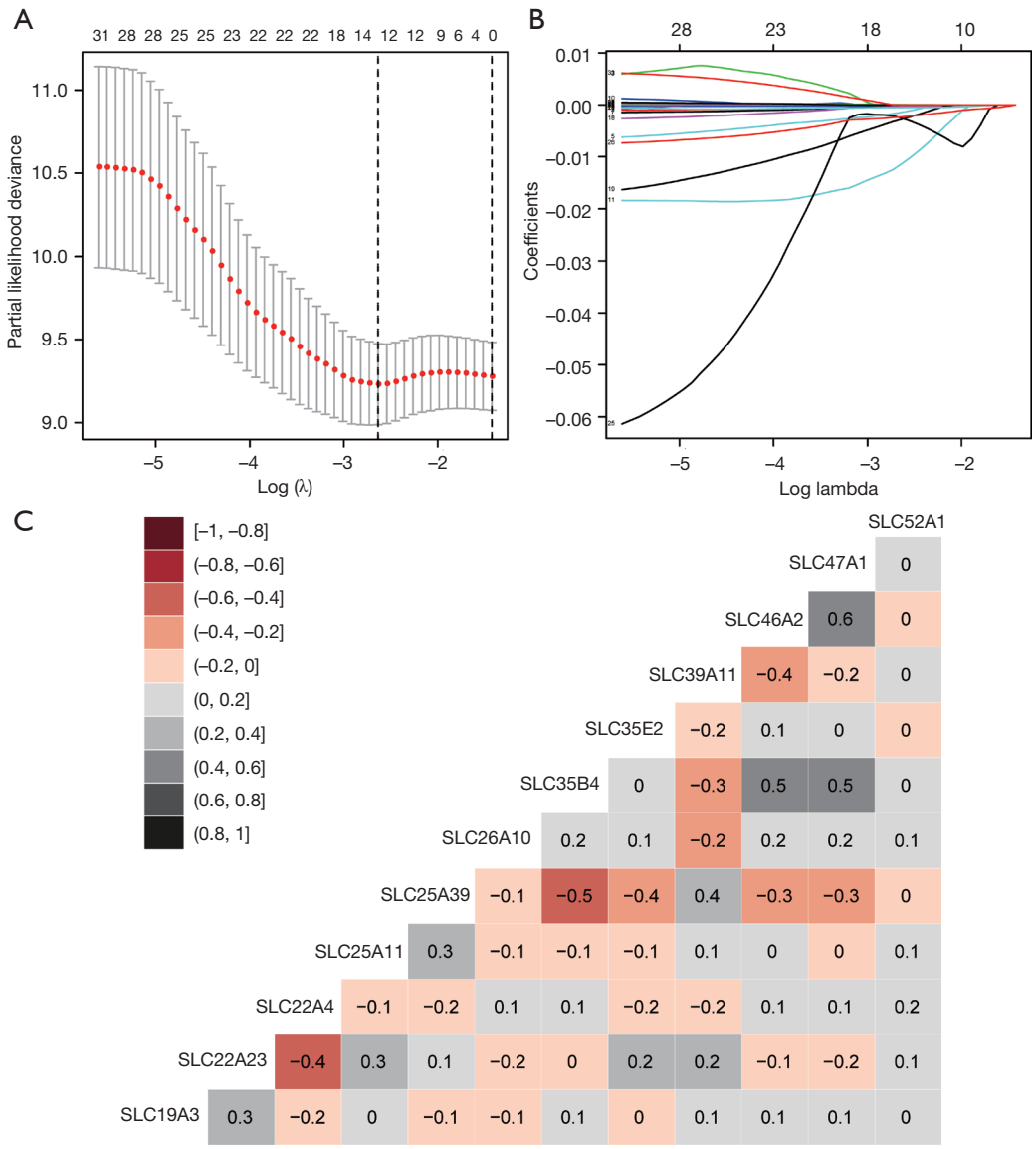

Figure 1 Matrix graphs of Pearson's correlation analysis of SLC genes. (A) LASSO regression analysis was used to screen 32 prognosis-related solute carrier family genes. Cross-validated error curve used to select optimal λ value according to partial likelihood deviance. Dotted vertical lines were produced at the optimal values according to the minimum criteria; (B) Coefficient profile plot of 33 parameters was drawn against the log (λ) sequence; (C) Matrix graphs of Pearson's correlation analysis of SLC family genes, the number in the matrix is the correlation coefficient between genes. LASSO, least absolute shrinkage and selection operator; SLC, solute carrier.

significantly higher expression in PDAC patients (Figure S3).

Joint-effect analysis and prognostic signature construction

According to the above study, we found that only *SLC19A3*, *SLC25A39*, and *SLC39A11* satisfied prognosis-related genes and differential expression in both the tumor and normal tissues. Thus, a joint-effect analysis and prognostic signature were comprised of *SLC19A3*, *SLC25A39*, and *SLC39A11*. In the joint-effect analysis, compared with Group A, Group III and Group 4 had the best prognosis in their large group (*Table 2*). We constructed a nomogram using clinical factors and the 3 SLC genes mentioned above which can be used to predict the 1-, 2-, and 3-year OS of PDAC patients (*Figure 4A*). The forest plot indicated that patients in

Table 1 Prognostic values of SLC genes expression in PDAC

Gene expression	Events/total (n=112)	MST (days)	Crude HR (95% CI)	Crude P value	Adjusted HR (95% CI)	Adjusted P value[a]
SLC19A3						
Low	39/56	449	1		1	
High	30/56	756	0.460 (0.276–0.766)	0.003	0.447 (0.250–0.800)	*0.007*
SLC22A23						
Low	43/56	497	1		1	
High	26/56	756	0.447 (0.272–0.732)	0.001	0.526 (0.289–0.956)	*0.035*
SLC22A4						
Low	38/56	506	1		1	
High	31/56	732	0.581 (0.357–0.945)	0.029	0.676 (0.397–1.151)	0.149
SLC25A11						
Low	38/56	554	1		1	
High	31/56	681	0.598 (0.368–0.971)	0.038	0.647 (0.382–1.096)	0.105
SLC25A39						
Low	30/56	748	1		1	
High	39/56	503	1.880 (1.153–3.065)	0.011	1.852 (1.071–3.202)	*0.027*
SLC26A10						
Low	43/56	549	1		1	
High	26/56	684	0.613 (0.375–1.003)	0.051	0.931 (0.528–1.641)	0.804
SLC35B4						
Low	37/56	504	1		1	
High	32/56	714	0.582 (0.356–0.953)	0.031	0.707 (0.402–1.244)	0.229
SLC35E2						
Low	42/56	534	1		1	
High	27/56	754	0.584 (0.356–0.955)	0.032	0.674 (0.401–1.133)	0.137
SLC39A11						
Low	32/56	705	1		1	
High	37/56	538	1.699 (1.046–2.761)	0.032	1.749 (1.017–3.009)	*0.043*
SLC46A2						
Low	37/56	524	1		1	
High	32/56	727	0.549 (0.336–0.895)	0.016	0.783 (0.454–1.350)	0.378
SLC47A1						
Low	39/56	459	1		1	
High	30/56	769	0.409 (0.249–0.670)	<0.001	0.504 (0.278–0.913)	*0.024*
SLC52A1						
Low	40/56	544	1		1	
High	29/56	688	0.611 (0.376–0.993)	0.047	0.774 (0.430–1.289)	0.292

Italic P values indicate statistically significant. [a], adjusted for histologic grade, radiation therapy, radical resection, and targeted molecular therapy. SLC, solute carrier; MST, median survival time; OS, overall survival; PDAC, pancreatic ductal adenocarcinoma; HR, hazard ratio; CI, confidence interval.

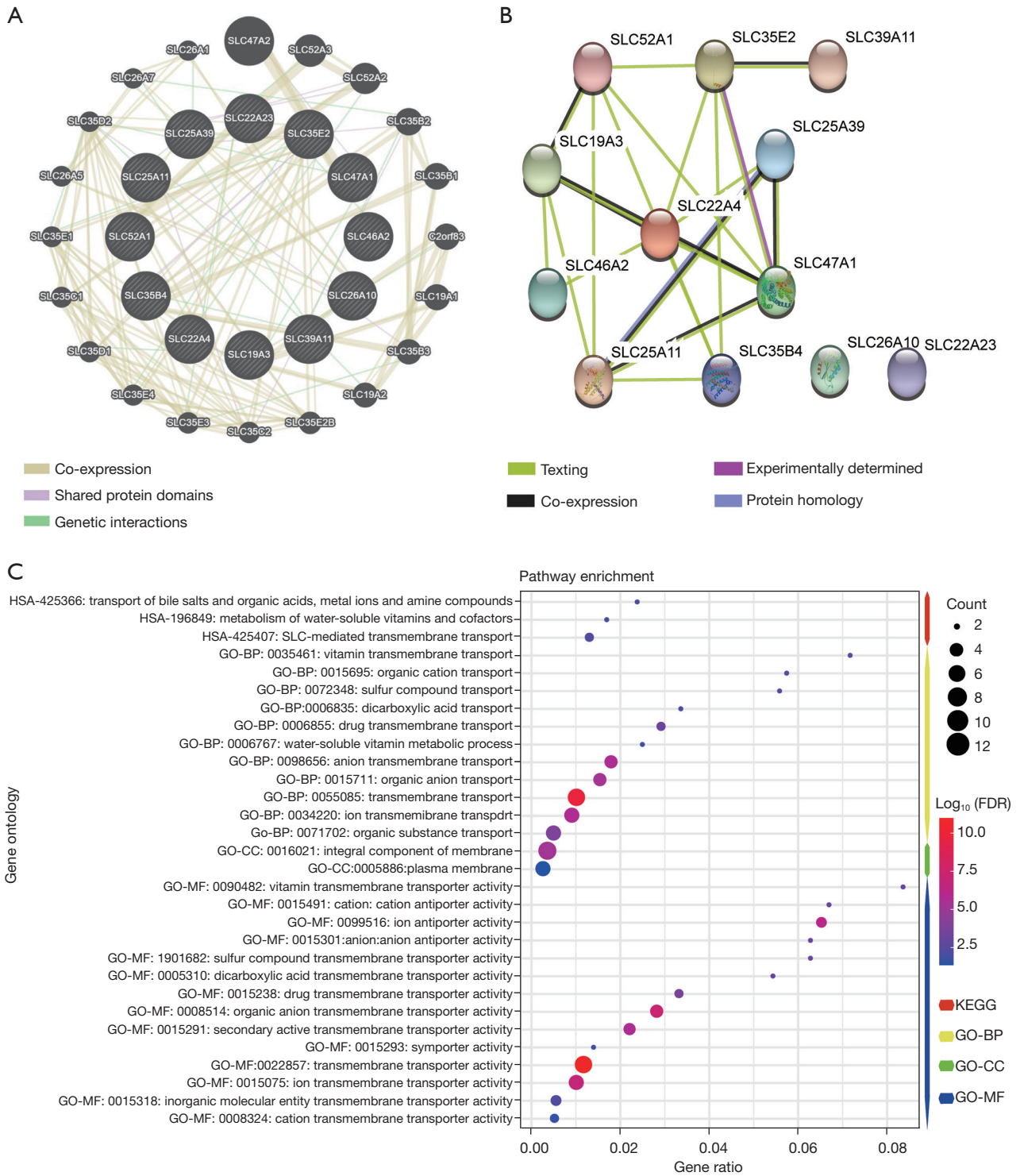

Figure 2 Interaction, KEGG pathway and GO term analysis of solute carrier family genes. (A) The gene-gene interaction networks of SLC genes from STRING; (B) the protein-protein interaction networks of SLC genes from GeneMANIA; (C) KEGG pathway and GO term analysis of SLC genes. KEGG, Kyoto Encyclopedia of Genes and Genomes; SLC, solute carrier; STRING, Search Tool for the Retrieval of Interacting Genes/proteins; GO, Gene Ontology.

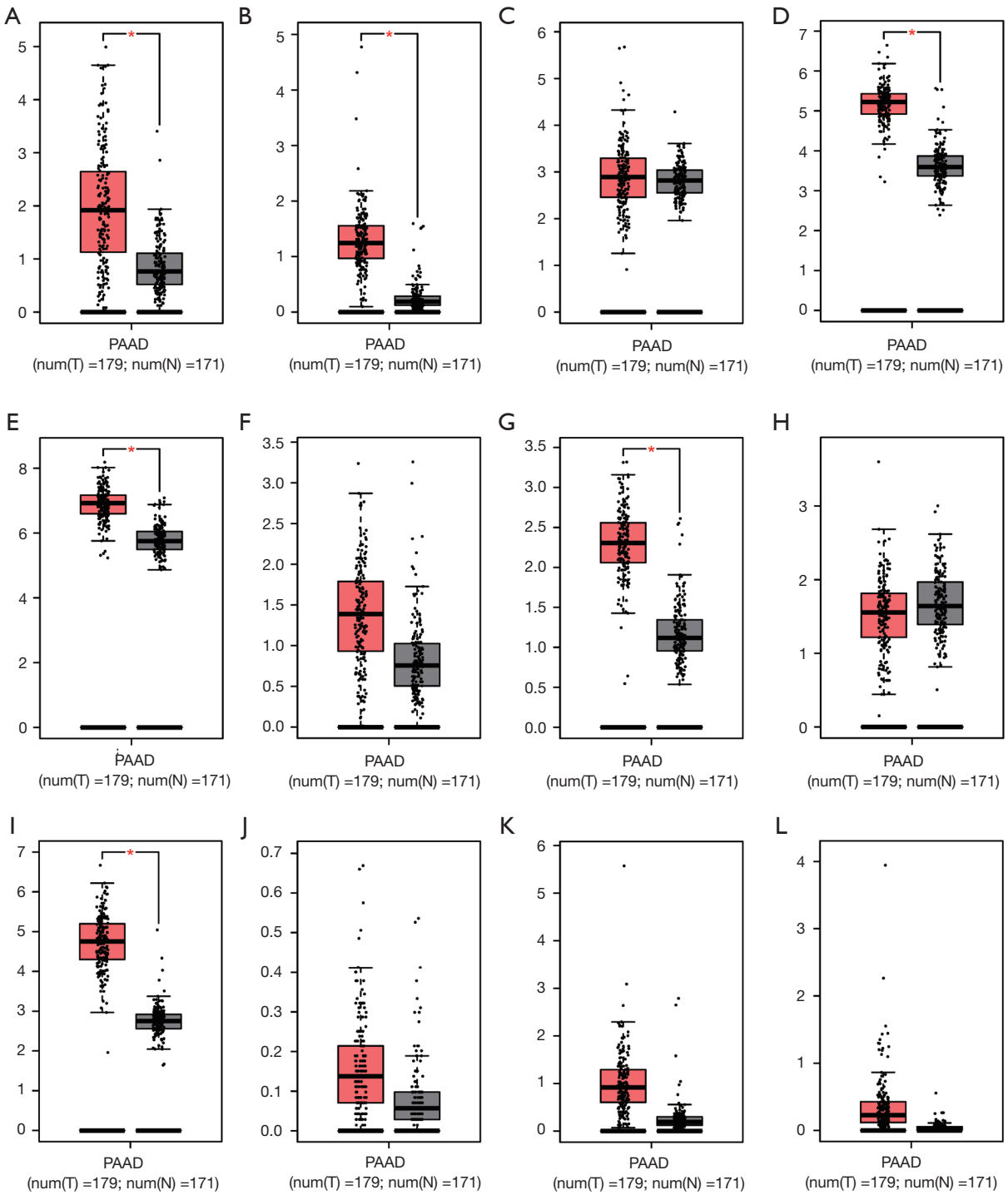

Figure 3 Gene expression level distribution of SLC genes in PAAD tissue and normal tissue. (A) *SLC19A3*; (B) *SLC22A4*; (C) *SLC22A3*; (D) *SLC25A11*; (E) *SLC25A39*; (F) *SLC26A10*; (G) *SLC35B4*; (H) *SLC35E2*; (I) *SLC39A11*; (J) *SLC46A2*; (K) *SLC47A1*; (L) *SLC52A1*. *, P<0.05. SLC, solute carrier; PAAD, pancreatic adenocarcinoma.

Table 2 Joint-effects survival analysis of SLC family genes expression levels with OS in patients

Group	*SLC19A3*	*SLC25A39*	*SLC39A11*	Patients	Number of events	MST	Crude HR (95% CI)	Crude P value	Adjusted HR (95% CI)	Adjusted P value[a]
A	Low	High	–	24	15	501	1		1	
B	Low	Low	–	32	24	407	1.272 (0.664–2.435)	0.469	1.229 (0.541–2.796)	0.622
C	High	Low	–	32	15	883	3.533 (1.730–7.215)	*0.001*	4.598 (1.948–10.851)	*<0.001*
D	High	High	–	24	15	592	1.549 (0.786–3.055)	0.206	1.797 (0.782–3.682)	0.181
I	Low	–	High	25	17	521	1		1	
II	Low	–	Low	31	22	373	0.531 (0.275–1.025)	0.057	0.511 (0.232–1.129)	0.097
III	High	–	Low	31	15	826	2.221 (1.063–4.639)	*0.034*	3.294 (1.265–8.574)	*0.015*
IV	High	–	High	25	15	652	1.269 (0.611–2.635)	0.523	1.216 (0.530–2.791)	0.645
1	–	Low	Low	42	21	773	1		1	
2	–	Low	High	14	9	630	0.671 (0.303–1.484)	0.324	0.705 (0.273–1.819)	0.47
3	–	High	Low	14	11	506	0.546 (0.257–1.159)	0.115	0.495 (0.215–1.139)	0.098
4	–	High	High	42	28	509	0.442 (0.245–0.797)	*0.007*	0.448 (0.225–0.891)	*0.022*

Italic P values indicate statistically significant. [a], adjusted for histologic grade, radiation therapy, radical resection, and targeted molecular therapy. SLC, solute carrier; MST, median survival time; OS, overall survival; PDAC, pancreatic ductal adenocarcinoma; HR, hazard ratio; CI, confidence interval.

the low-risk group had a significantly better prognosis than the high-risk group under the following conditions: young patients (young patients condit alcohol history, high histologic grade (G3 + G4), no radical resection, no radiation therapy, and those who received targeted macular therapy (*Figure 4B*).

The prognostic signature model, which included *SLC19A3*, *SLC25A39*, and *SLC39A11* for OS is shown in *Figure 5A*. The prognosis of the high-risk group was significantly worse than that of the low-risk group (778 *vs.* 478 days; P=0.001). The risk score, survival status, and heatmap are presented from top to bottom. The ROC curves for predicting the OS of PDAC patients according to SLCs and risk score showed diagnostic value. The area under the curve (AUC) of *SLC19A3* for predicting the 1-, 2-, and 3-year survival was 62.2%, 73.3%, and 74.1%, respectively, which was the highest among the genes (*Figure 5B*).

The situation of immune infiltration

After CIBERSORT calculations, 63 out of 112 PDAC samples with P values <0.05 were included in the subsequent analyses. Since the percentage of eosinophils and gamma delta T cells could not be counted, 20 types of immune cells in 63 PDAC samples were analyzed. The proportion of 20 types of immune cells in each sample and a heat map of the immune cells are presented in *Figure 6A*,*6B*. Naïve B cells and M2 macrophages were moderately negatively correlated. The proportion of memory B cells (P=0.004), naive B cells (P=0.007), CD8 T cells (P=0.003), activated memory CD4 T cells (P=0.004), and activated NK cells (P=0.019) were significantly higher in the low-risk group compared to that of the high-risk group. In contrast, the proportion of follicular helper T cells (P<0.001), regulatory T cells (Tregs) (P=0.005), M0 macrophages (P<0.001), and M2 macrophages (P=0.017) were higher in the high-risk group (*Figure 6C*). The Pearson's correlation coefficient was presented in the matrix box of the correlation graph, and activated natural killer (NK) cells and regulatory T cells (Tregs), naïve CD4 T cells, and memory B cells constituted the median and were moderately positively correlated (*Figure 7*).

GSEA

In the ROC curves, *SLC19A3* was the most eye-catching gene with a high AUC. Therefore, the potential mechanisms associated with the level of *SLC19A3* expression on the prognosis of patients with pancreatic

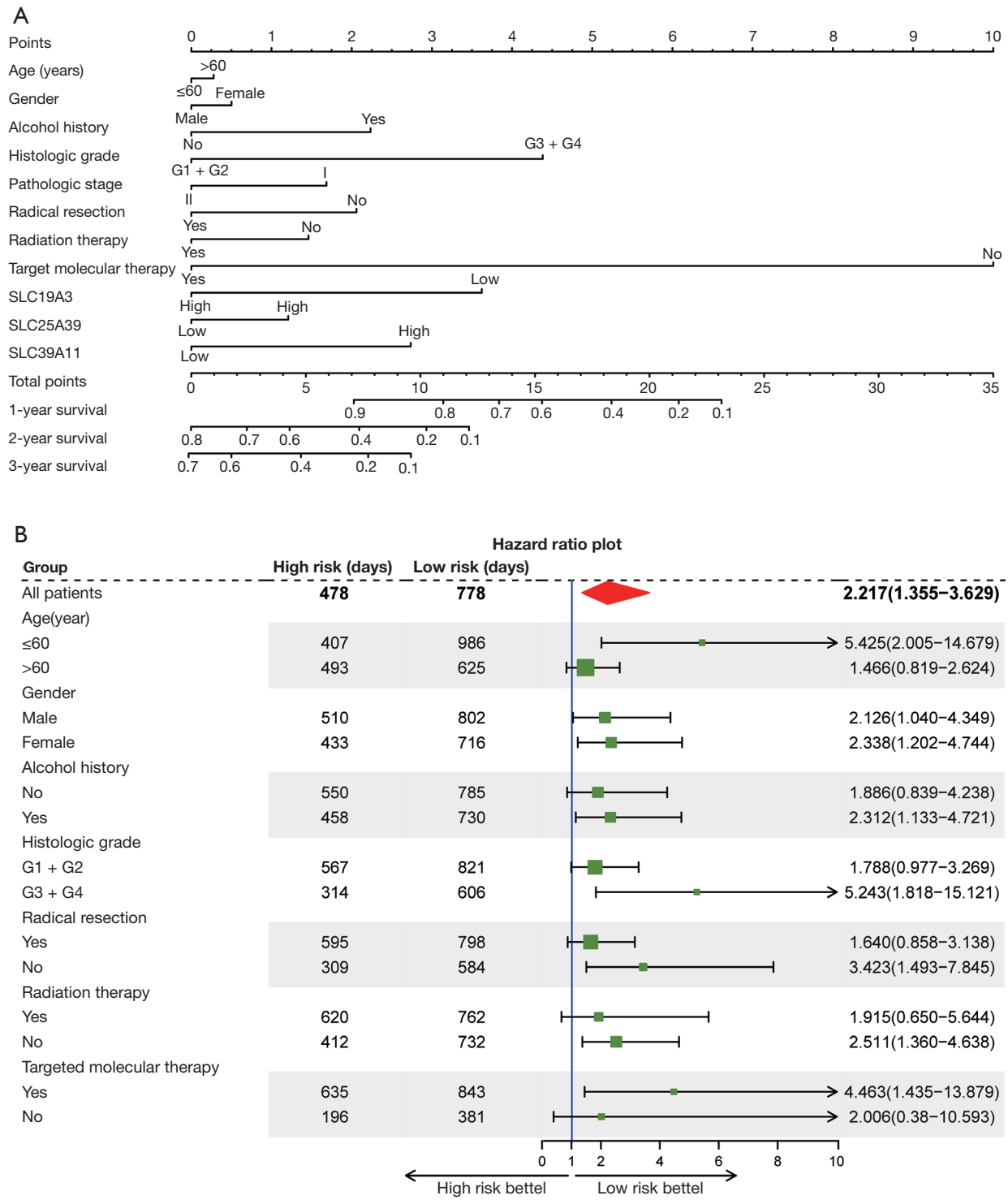

Figure 4 Prognosis nomogram for predicting overall survival and forest-plot for subgroup analysis. (A) Nomogram for PDAC patient 1-, 2-, and 3-year OS prediction; (B) Forest plot for demonstrating the relationship between subgroups of prognostic signatures and clinical factors. PDAC, pancreatic ductal adenocarcinoma; OS, overall survival.

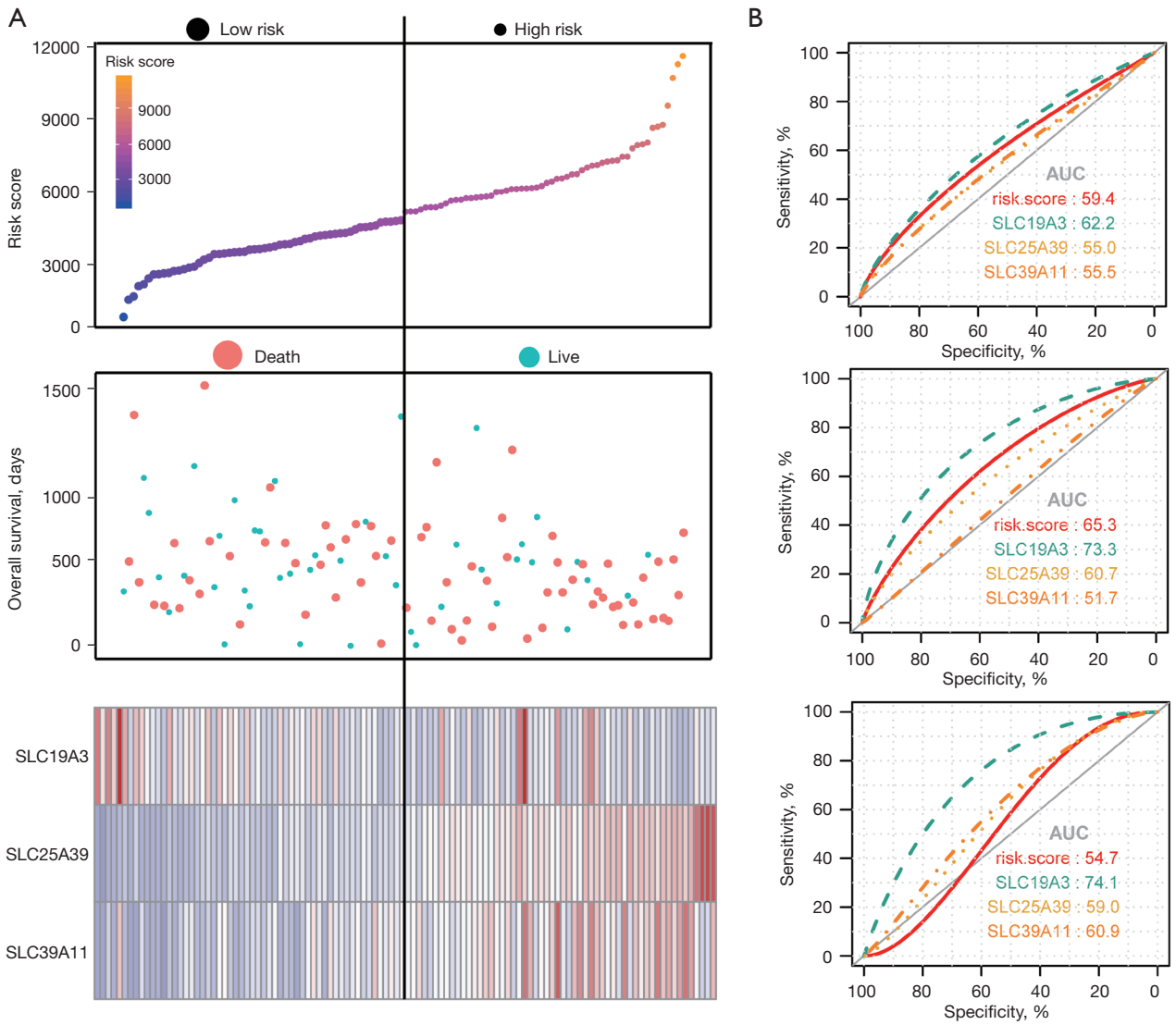

Figure 5 Expression model constructed using risk score, *SLC19A3*, *SLC25A39*, and *SLC39A11* expression in early-stage PDAC. (A) From top to bottom; risk score plot, survival status scatter plot and heat map of the expression levels of *SLC19A3*, *SLC25A39*, and *SLC39A11* in low- and high-risk groups; (B) from top to bottom: ROC curve for predicting 1-year survival in patients with early-stage PDAC by *SLC19A3*, *SLC25A39*, *SLC39A11* and risk score; ROC curve for predicting 2-year survival in patients with early-stage PDAC by *SLC19A3*, *SLC25A39*, *SLC39A11* and risk score; ROC curve for predicting 3-year survival in patients with early-stage PDAC by *SLC19A3*, *SLC25A39*, *SLC39A11* and risk score. PDAC, pancreatic ductal adenocarcinoma; ROC, receiver operating characteristic.

cancer were explored in GSEA. In the c2 gene set, the low *SLC19A3* expression group was enriched for genes in the cell cycle, base excision repair, DNA replication, MYC active pathway, WNT signaling pathway, and p53 signaling pathway (*Figure 8A*). The c5 gene set results suggested that base excision repair, cell cycle checkpoint, damaged DNA binding, DNA replication, DNA damage checkpoint, and DNA integrity checkpoint were the main associated functions (*Figure 8B*).

Discussion

In this study, we performed both a survival and bioinformatic analysis using high-throughput RNA-sequencing data obtained from TCGA. In the survival analysis, the expression of *SLC19A3*, *SLC25A39*, and

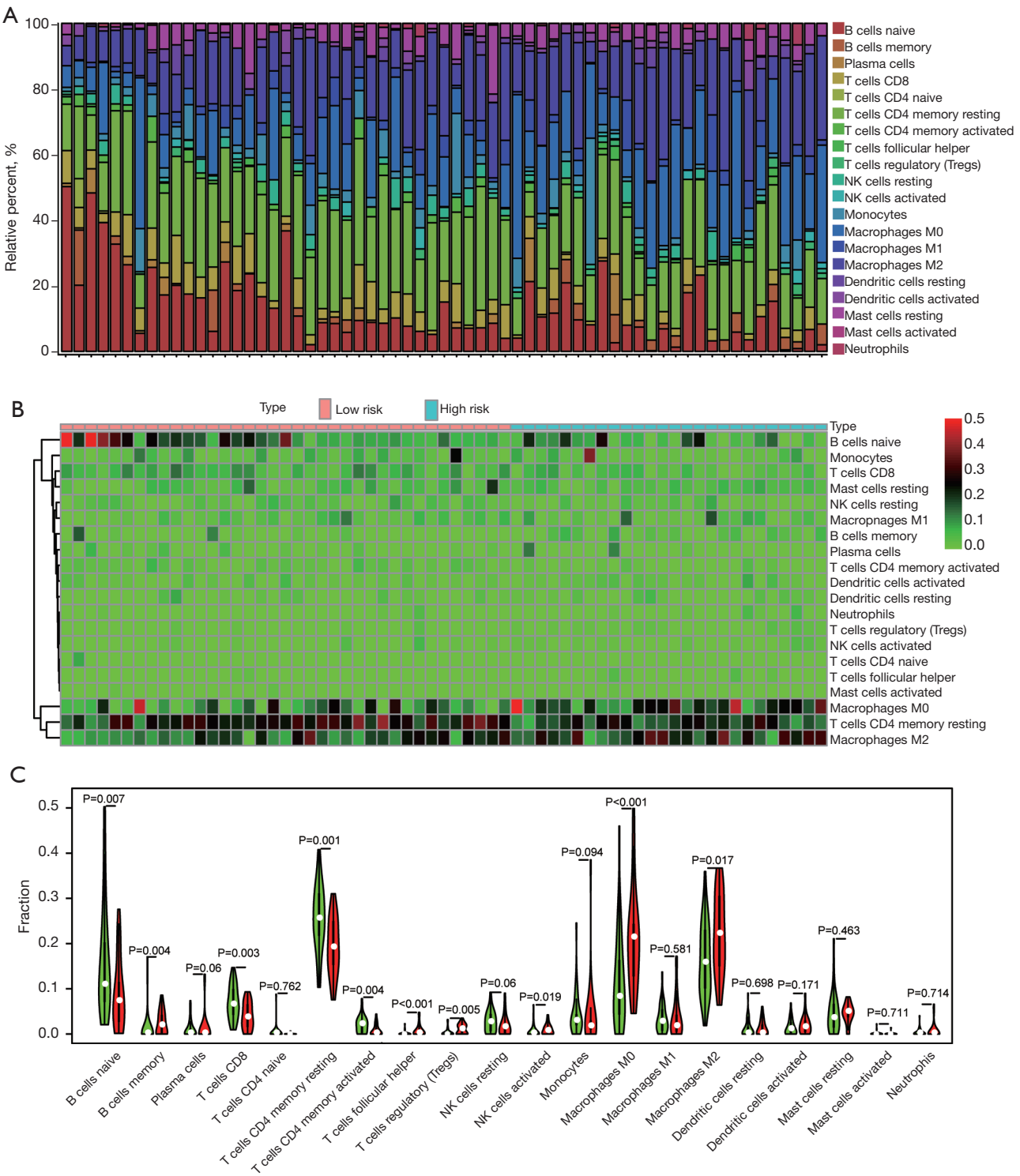

Figure 6 The landscape of tumor-infiltrating immune cells for 112 early-stage PDAC cases. (A) Histogram showing 20 types of TIILs in each case; (B) Heat map for infraction of 20 types of TIILs in each case and different groups; (C) comparison of the immune cell fractions between tumor tissues of the high-risk group and low-risk groups. PDAC, pancreatic ductal adenocarcinoma; TIILs, tumor-infiltrating immune cells.

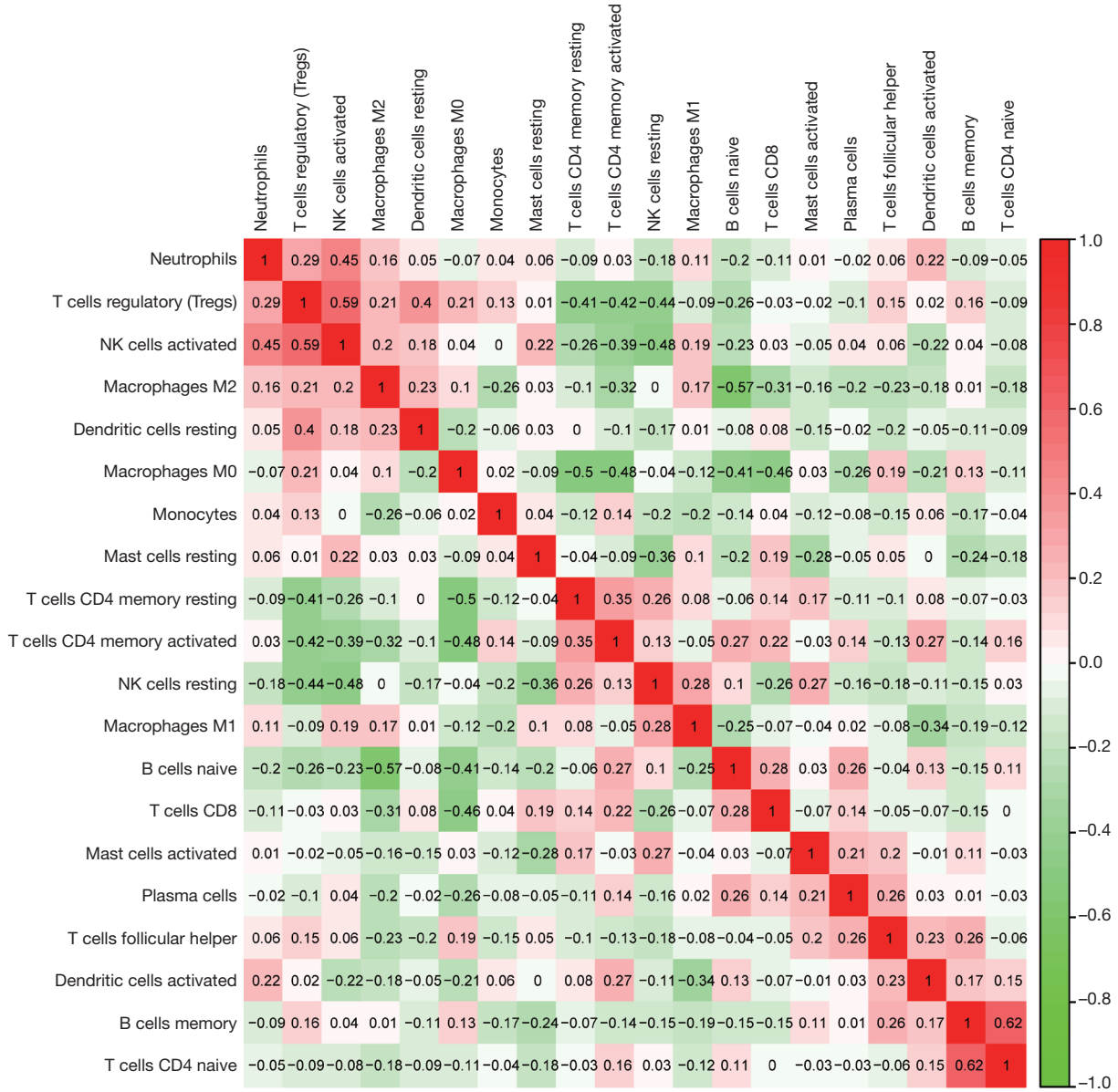

Figure 7 Matrix graphs of Pearson's correlation analysis of 20 types of immune cells.

SLC39A11 was found to have the ability to significantly affect the prognosis of PDAC patients; however, the expression of *SLC19A3* was completely opposite to that of *SLC25A39* and *SLC39A11*, and overexpression led to a better patient prognosis. This finding is also consistent with previous research. In particular, *SLC5A8* also acted as a tumor suppressor gene, and *SLC7A11* inhibited pancreatic carcinoma via the PI3K/Akt signaling pathway (39,40). However high *SLC28A1* expression indicated a worse prognosis, and *SLC22A3* and *SLC29A3* affected the therapeutic effect of nucleoside drugs in PC (41). Due to the substantial heterogeneity of both tumors and individuals, a single gene often cannot reflect the effect of the level of gene expression on the prognosis of PDAC. Hence, we constructed a prognostic signature and genetic risk score model to assess the prognosis. In addition, the forest plot showed some differences in clinical factors and patient sensitivity to certain treatment modalities. For example, in the context that radiotherapy can indeed prolong the OS of patients, patients in the low-risk group did not receive

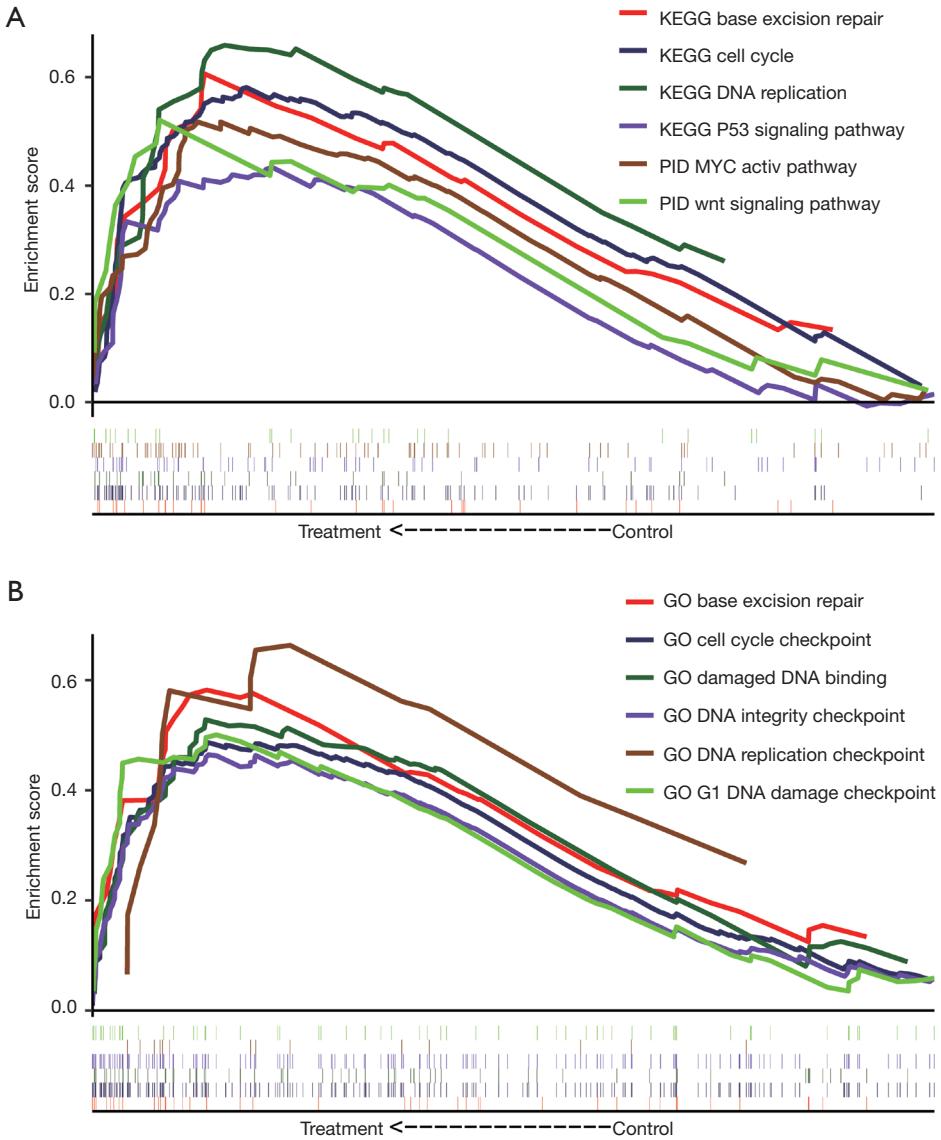

Figure 8 GSEA results for *SLC19A3* in patients with PDAC. (A) GSEA results of C2 gene sets for *SLC19A3*; (B) GSEA results of C5 gene sets for *SLC19A3*. GSEA, gene set enrichment analysis; PDAC, pancreatic ductal adenocarcinoma; KEGG, Kyoto Encyclopedia of Genes and Genomes; GO, Gene Ontology.

radiotherapy, and the OS was similar to those who received radiotherapy. Therefore, we believe that our prognostic signature could predict the prognosis and also provide some evidence for clinical decision-making. In our ROC curves and nomogram, all 3 genes showed excellent efficacy for predicting the prognosis, of which *SLC19A3* was the most remarkable. Therefore, we inferred that the 3 genes were independent prognostic factors for PDAC patients.

In most of the previous research, variation of *SLC19A3* lead to a thiamine deficiency and resulted in certain genetic disorders, including biotin thiamine responsive basal ganglia disease (BTRBGD), Leigh syndrome, and mitochondrial disorders (42,43). Thiamine transporter-2 (ThTR-2, encoded by *SLC19A3*) is a specific transporter that plays a role in small intestinal absorption and cellular uptake when thiamine is a critical cofactor for nucleic acid synthesis (44,45). These conclusions are also consistent with our GSEA findings that *SLC19A3* participates in the cell cycle, DNA replication, and DNA damage checkpoints. In addition, diabetes is a proven risk factor for PC, and

metformin is an effective oral medicine. A study conducted by Liang *et al.* reported that metformin was a substrate of thiamine transporters and that inhibiting ThTR-2 could reduce the uptake of metformin (5,46). Similarly, cigarette smoking is also a well-known risk factor. Srinivasan *et al.* reported that chronic nicotine exposure inhibited the uptake of thiamin, as well as the level of ThTR-2 and *SLC19A3* expression in pancreatic acinar cells (47). Furthermore, a breast cancer (BC) study performed by Liu *et al.* reported that the down-regulation of gene expression contributes to the resistance of tumor cells to apoptosis (48). The above results indicate that the level of *SLC19A3* expression can affect prognosis and is also associated with the risk factors of PC. Thus, *SLC19A3* could act as a new tumor suppressor in PDAC.

We also investigated the potential mechanism of *SLC19A3* on PC by GSEA. The results showed that the expression of *SLC19A3* was associated with cell cycle, DNA replication, DNA damage, and integrity checkpoints. These findings indicate that *SLC19A3* may be involved in the transportation of substances during DNA synthesis and replication to ensure normal gene replication. In addition, the low expression of *SLC19A3* is enriched in the MYC and *p53* signaling pathways, which are considered the key mutation signaling pathways in PC (49,50).

Mutation of *p53* is one of the most common genetic mutations in tumors, and it has been reported that *p53* is missing or mutated in approximately 75% of PDAC patients (51). In a mouse model of PDAC, the presence of *KRAS* and the loss of *p53* resulted in a loss in autophagy that did not stop tumor progression but actually accelerated tumor progression (52). Therefore, a lack of *SLC19A3* was associated with the *p53* signaling pathway, and finally resulted in the loss of autophagy and progression of PDAC.

Some researchers have demonstrated that transcriptomic analysis can be used to explore the immune infiltration microenvironment (53). Tumor-recruited M2 macrophages promote gastric and breast cancer metastasis via M2 macrophage secreted CHI3L1 protein, and it was one the mechanism of M2 macrophages leading to poor prognosis (54). CD8 T cells, CD4 T cells, and NK cells could inhibit tumor progression and metastasis through cytotoxic effects (55). Different types of immune cells also have different effects on tumor progression. For example, cytotoxic CD8 T cells and CD4 helper T cells can inhibit tumor progression, and a high level of activated CD8 T cells can prolong the prognosis of patients (56). In contrast, macrophages, mast cells, and neutrophils can promote tumor progression and are not conducive to the patient's prognosis (56). We analyzed the situation of TIICS in both high- and low-risk groups using CIBERSORT and found that the TICCs favorable to prognosis (e.g., CD8 T cells, CD4 T cells, and NK cells) were significantly higher in the low-risk group. Simultaneously, M0 and M2 macrophages, which have been found to be less favorable for prognosis were significantly higher in the high-risk group. Immunotherapy including immune checkpoint blockade is not effective in PDAC (57). Therefore, there is an urgent need for new immunotherapy targets to improve the prognosis of patients in PDAC. A recent report demonstrated that the selective targeting of MHC-I molecules for degradation could enhance autophagy and leads to an improved therapeutic strategy (58). It is known that autophagy and apoptosis are indispensable steps in immunotherapy, as well as the suppression of tumorigenesis and progression. Moreover, some SLCs have been shown to participate in glucose uptake and lactate release, as well as the promotion phagocyte engulfment of apoptotic cells (59). In addition, SLC genes can modify dendritic cells and induce an anti-gastric cancer immune response (60). Therefore, SLCs may be a potential target of PDAC immunotherapy, which can promote patient prognosis in the high-risk patient group.

Previous studies on SLCs have suggested that the level of SLC expression is related to the prognosis of certain tumors. For example, *SLC39A7*, *SLC39A11*, and *SLC39A14* have been associated with the prognosis in GC, and the co-expression of *SLC1A5*, *SLC7A5*, and *SLC3A2* has been shown to affect aggressive BC which is driven by c-MYC (61,62). However, we first pointed out that *SLC19A3*, *SLC25A39*, and *SLC39A11* were significantly associated with the prognosis of PDAC, and the potential mechanisms were explored. A prognostic signature was proposed when immunotherapy did not have a good effect on PDAC, and it was calculated that TIICS differed between the high- and low-risk groups. These findings are promising for providing new targets for treatment and biomarkers for predicting the prognosis of PDAC patients.

This study had several limitations. First, the analysis involved publicly available data, and thus, information for some patients was missing (e.g., the patient's medication, and immune-related medical history), which prevented us from performing further research on these patients. Second, although we established strict inclusion and exclusion criteria, our research was based on a bioinformatics analysis. Therefore, the obtained results still require further

experimental verification. Third, due to the difficulty in obtaining PDAC tumor tissue, the level of messenger (mRNA) expression for some SLCs was derived from a single cohort, and a verification cohort was lacking. Fourth, in order to enhance the credibility of these results, we established strict standards, which also led to a small number of samples. A larger sample size is required to minimize bias in future studies.

Despite these limitations, this was the first study to report that *SLC19A3*, *SLC25A35*, and *SLC39A11* and the prognosis of PDAC patients are significantly correlated. The mechanism by which *SLC19A3* expression affects PDAC and the differences in tumor infiltrating cells within the tumor were explored using GSEA and CIBERSORT, respectively. Upon future confirmation of these conclusions, *SLC19A3* may represent a new PDAC tumor suppressor that can contribute to the management and treatment of PDAC patients.

Conclusions

The *SLC19A3*, *SLC25A35*, and *SLC39A11* genes are significantly associated with the prognosis of PDAC patients and may act as a potential biomarker for predicting the prognosis of PDAC following a pancreaticoduodenectomy. The *SLC19A3* gene may represent a tumor suppressor in PDAC and affect tumor development and progression through the *MYC* and *p53* signaling pathways and changes in immune cell infiltration. However, these findings should be verified through future functional experiments.

Acknowledgments

Funding: None.

Footnote

Reporting Checklist: The authors have completed the TRIPOD reporting checklist. Available at https://atm.amegroups.com/article/view/10.21037/atm-21-6341/rc

Conflicts of Interest: All authors have completed the ICMJE uniform disclosure form (available at https://atm.amegroups.com/article/view/10.21037/atm-21-6341/coif). The authors have no conflicts of interest to declare.

Ethical Statement: The authors are accountable for all aspects of the work in ensuring that questions related to the accuracy or integrity of any part of the work are appropriately investigated and resolved. The study was conducted in accordance with the Declaration of Helsinki (as revised in 2013).

References

1. Lin QJ, Yang F, Jin C, et al. Current status and progress of pancreatic cancer in China. World J Gastroenterol 2015;21:7988-8003.
2. Raimondi S, Maisonneuve P, Lowenfels AB. Epidemiology of pancreatic cancer: an overview. Nat Rev Gastroenterol Hepatol 2009;6:699-708.
3. Bray F, Ferlay J, Soerjomataram I, et al. Global cancer statistics 2018: GLOBOCAN estimates of incidence and mortality worldwide for 36 cancers in 185 countries. CA Cancer J Clin 2018;68:394-424.
4. Gillen S, Schuster T, Meyer Zum Büschenfelde C, et al. Preoperative/neoadjuvant therapy in pancreatic cancer: a systematic review and meta-analysis of response and resection percentages. PLoS Med 2010;7:e1000267.
5. Kamisawa T, Wood LD, Itoi T, et al. Pancreatic cancer. Lancet 2016;388:73-85.
6. Tang K, Lu W, Qin W, et al. Neoadjuvant therapy for patients with borderline resectable pancreatic cancer: A systematic review and meta-analysis of response and resection percentages. Pancreatology 2016;16:28-37.
7. Siegel R, Ma J, Zou Z, et al. Cancer statistics, 2014. CA Cancer J Clin 2014;64:9-29.
8. Schaller L, Lauschke VM. The genetic landscape of the human solute carrier (SLC) transporter superfamily. Hum Genet 2019;138:1359-77.
9. Cedernaes J, Olszewski PK, Almén MS, et al. Comprehensive analysis of localization of 78 solute carrier genes throughout the subsections of the rat gastrointestinal tract. Biochem Biophys Res Commun 2011;411:702-7.

10. Mäkelä S, Kere J, Holmberg C, et al. SLC26A3 mutations in congenital chloride diarrhea. Hum Mutat 2002;20:425-38.
11. Al-Suyufi Y, ALSaleem K, Al-Mehaidib A, et al. SLC5A1 Mutations in Saudi Arabian Patients With Congenital Glucose-Galactose Malabsorption. J Pediatr Gastroenterol Nutr 2018;66:250-2.
12. Cannizzaro M, Jarošová J, De Paepe B. Relevance of solute carrier family 5 transporter defects to inherited and acquired human disease. J Appl Genet 2019;60:305-17.
13. Li H, Myeroff L, Smiraglia D, et al. SLC5A8, a sodium transporter, is a tumor suppressor gene silenced by methylation in human colon aberrant crypt foci and cancers. Proc Natl Acad Sci U S A 2003;100:8412-7.
14. Gamble LD, Purgato S, Murray J, et al. Inhibition of polyamine synthesis and uptake reduces tumor progression and prolongs survival in mouse models of neuroblastoma. Sci Transl Med 2019;11:eaau1099.
15. Girardi E, César-Razquin A, Lindinger S, et al. A widespread role for SLC transmembrane transporters in resistance to cytotoxic drugs. Nat Chem Biol 2020;16:469-78.
16. Lemstrová R, Souček P, Melichar B, et al. Role of solute carrier transporters in pancreatic cancer: a review. Pharmacogenomics 2014;15:1133-45.
17. Sprowl JA, Ness RA, Sparreboom A. Polymorphic transporters and platinum pharmacodynamics. Drug Metab Pharmacokinet 2013;28:19-27.
18. Zhou J, Hui X, Mao Y, et al. Identification of novel genes associated with a poor prognosis in pancreatic ductal adenocarcinoma via a bioinformatics analysis. Biosci Rep 2019;39:BSR20190625.
19. Schulz M, Salamero-Boix A, Niesel K, et al. Microenvironmental Regulation of Tumor Progression and Therapeutic Response in Brain Metastasis. Front Immunol 2019;10:1713.
20. Quail DF, Joyce JA. Microenvironmental regulation of tumor progression and metastasis. Nat Med 2013;19:1423-37.
21. Fan JQ, Wang MF, Chen HL, et al. Current advances and outlooks in immunotherapy for pancreatic ductal adenocarcinoma. Mol Cancer 2020;19:32.
22. Robert C, Long GV, Brady B, et al. Nivolumab in previously untreated melanoma without BRAF mutation. N Engl J Med 2015;372:320-30.
23. Ansell SM, Lesokhin AM, Borrello I, et al. PD-1 blockade with nivolumab in relapsed or refractory Hodgkin's lymphoma. N Engl J Med 2015;372:311-9.
24. Kang YK, Boku N, Satoh T, et al. Nivolumab in patients with advanced gastric or gastro-oesophageal junction cancer refractory to, or intolerant of, at least two previous chemotherapy regimens (ONO-4538-12, ATTRACTION-2): a randomised, double-blind, placebo-controlled, phase 3 trial. Lancet 2017;390:2461-71.
25. Brahmer JR, Tykodi SS, Chow LQ, et al. Safety and activity of anti-PD-L1 antibody in patients with advanced cancer. N Engl J Med 2012;366:2455-65.
26. Group Young Researchers In Inflammatory Carcinogenesis, Wandmacher AM, Mehdorn AS, Sebens S. The Heterogeneity of the Tumor Microenvironment as Essential Determinant of Development, Progression and Therapy Response of Pancreatic Cancer. Cancers (Basel) 2021;13:4932.
27. Kiryu S, Ito Z, Suka M, et al. Prognostic value of immune factors in the tumor microenvironment of patients with pancreatic ductal adenocarcinoma. BMC Cancer 2021;21:1197.
28. Ansari RE, Craze ML, Althobiti M, et al. Enhanced glutamine uptake influences composition of immune cell infiltrates in breast cancer. Br J Cancer 2020;122:94-101.
29. Yip SH, Wang P, Kocher JA, et al. Linnorm: improved statistical analysis for single cell RNA-seq expression data. Nucleic Acids Res 2017;45:e179.
30. Liao X, Huang K, Huang R, et al. Genome-scale analysis to identify prognostic markers in patients with early-stage pancreatic ductal adenocarcinoma after pancreaticoduodenectomy. Onco Targets Ther 2017;10:4493-506.
31. Tang Z, Li C, Kang B, et al. GEPIA: a web server for cancer and normal gene expression profiling and interactive analyses. Nucleic Acids Res 2017;45:W98-W102.
32. Szklarczyk D, Franceschini A, Wyder S, et al. STRING v10: protein-protein interaction networks, integrated over the tree of life. Nucleic Acids Res 2015;43:D447-52.
33. Warde-Farley D, Donaldson SL, Comes O, et al. The GeneMANIA prediction server: biological network integration for gene prioritization and predicting gene function. Nucleic Acids Res 2010;38:W214-20.
34. Gentles AJ, Newman AM, Liu CL, et al. The prognostic landscape of genes and infiltrating immune cells across human cancers. Nat Med 2015;21:938-45.
35. Newman AM, Liu CL, Green MR, et al. Robust enumeration of cell subsets from tissue expression profiles. Nat Methods 2015;12:453-7.

36. Subramanian A, Tamayo P, Mootha VK, et al. Gene set enrichment analysis: a knowledge-based approach for interpreting genome-wide expression profiles. Proc Natl Acad Sci U S A 2005;102:15545-50.
37. Liberzon A, Birger C, Thorvaldsdóttir H, et al. The Molecular Signatures Database (MSigDB) hallmark gene set collection. Cell Syst 2015;1:417-25.
38. François O, Martins H, Caye K, et al. Controlling false discoveries in genome scans for selection. Mol Ecol 2016;25:454-69.
39. Park JY, Helm JF, Zheng W, et al. Silencing of the candidate tumor suppressor gene solute carrier family 5 member 8 (SLC5A8) in human pancreatic cancer. Pancreas 2008;36:e32-9.
40. Zhu JH, De Mello RA, Yan QL, et al. MiR-139-5p/SLC7A11 inhibits the proliferation, invasion and metastasis of pancreatic carcinoma via PI3K/Akt signaling pathway. Biochim Biophys Acta Mol Basis Dis 2020;1866:165747.
41. Mohelnikova-Duchonova B, Brynychova V, Hlavac V, et al. The association between the expression of solute carrier transporters and the prognosis of pancreatic cancer. Cancer Chemother Pharmacol 2013;72:669-82.
42. Pronicka E, Piekutowska-Abramczuk D, Ciara E, et al. New perspective in diagnostics of mitochondrial disorders: two years' experience with whole-exome sequencing at a national paediatric centre. J Transl Med 2016;14:174.
43. Ortigoza-Escobar JD, Alfadhel M, Molero-Luis M, et al. Thiamine deficiency in childhood with attention to genetic causes: Survival and outcome predictors. Ann Neurol 2017;82:317-30.
44. Asencio C, Rodríguez-Hernandez MA, Briones P, et al. Severe encephalopathy associated to pyruvate dehydrogenase mutations and unbalanced coenzyme Q10 content. Eur J Hum Genet 2016;24:367-72.
45. Ah Mew N, Loewenstein JB, Kadom N, et al. MRI features of 4 female patients with pyruvate dehydrogenase E1 alpha deficiency. Pediatr Neurol 2011;45:57-9.
46. Liang X, Chien HC, Yee SW, et al. Metformin Is a Substrate and Inhibitor of the Human Thiamine Transporter, THTR-2 (SLC19A3). Mol Pharm 2015;12:4301-10.
47. Srinivasan P, Thrower EC, Loganathan G, et al. Chronic Nicotine Exposure In Vivo and In Vitro Inhibits Vitamin B1 (Thiamin) Uptake by Pancreatic Acinar Cells. PLoS One 2015;10:e0143575.
48. Liu S, Huang H, Lu X, et al. Down-regulation of thiamine transporter THTR2 gene expression in breast cancer and its association with resistance to apoptosis. Mol Cancer Res 2003;1:665-73.
49. English IA, Sears RC. Deconstructing Pancreatic Adenocarcinoma by Targeting the Conductor, MYC. Cancer Discov 2020;10:495-7.
50. Ogawa S, Fukuda A, Matsumoto Y, et al. SETDB1 Inhibits p53-Mediated Apoptosis and Is Required for Formation of Pancreatic Ductal Adenocarcinomas in Mice. Gastroenterology 2020;159:682-696.e13.
51. Nigro JM, Baker SJ, Preisinger AC, et al. Mutations in the p53 gene occur in diverse human tumour types. Nature 1989;342:705-8.
52. Rosenfeldt MT, O'Prey J, Morton JP, et al. p53 status determines the role of autophagy in pancreatic tumour development. Nature 2013;504:296-300.
53. Teschendorff AE, Miremadi A, Pinder SE, et al. An immune response gene expression module identifies a good prognosis subtype in estrogen receptor negative breast cancer. Genome Biol 2007;8:R157.
54. Chen Y, Zhang S, Wang Q, et al. Tumor-recruited M2 macrophages promote gastric and breast cancer metastasis via M2 macrophage-secreted CHI3L1 protein. J Hematol Oncol 2017;10:36.
55. Ravindranath MH, Filippone EJ, Devarajan A, et al. Enhancing Natural Killer and CD8+ T Cell-Mediated Anticancer Cytotoxicity and Proliferation of CD8+ T Cells with HLA-E Monospecific Monoclonal Antibodies. Monoclon Antib Immunodiagn Immunother 2019;38:38-59.
56. Fridman WH, Pagès F, Sautès-Fridman C, et al. The immune contexture in human tumours: impact on clinical outcome. Nat Rev Cancer 2012;12:298-306.
57. O'Reilly EM, Oh DY, Dhani N, et al. Durvalumab With or Without Tremelimumab for Patients With Metastatic Pancreatic Ductal Adenocarcinoma: A Phase 2 Randomized Clinical Trial. JAMA Oncol 2019;5:1431-8.
58. Yamamoto K, Venida A, Yano J, et al. Autophagy promotes immune evasion of pancreatic cancer by degrading MHC-I. Nature 2020;581:100-5.
59. Morioka S, Perry JSA, Raymond MH, et al. Efferocytosis induces a novel SLC program to promote glucose uptake and lactate release. Nature 2018;563:714-8.
60. Xue G, Cheng Y, Ran F, et al. SLC gene-modified dendritic cells mediate T cell-dependent anti-gastric cancer immune responses in vitro. Oncol Rep 2013;29:595-604.
61. Ding B, Lou W, Xu L, et al. Analysis the prognostic values

of solute carrier (SLC) family 39 genes in gastric cancer. Am J Transl Res 2019;11:486-98.
62. El-Ansari R, Craze ML, Alfarsi L, et al. The combined expression of solute carriers is associated with a poor prognosis in highly proliferative ER+ breast cancer. Breast Cancer Res Treat 2019;175:27-38.

(English Language Editor: J. Jones)

Cite this article as: Meng Y, Li Y, Fang D, Huang Y. Identification of solute carrier family genes related to the prognosis and tumor-infiltrating immune cells of pancreatic ductal adenocarcinoma. Ann Transl Med 2022;10(2):57. doi: 10.21037/atm-21-6341

Supplementary

Table S1 The result of prognostic value of clinical variables[a]

Variables	Event of patients (n=112)	OS		
		MST (days)	HR (95% CI)	P value
Age (years)				
≤60	20/38	775.1	1	
>60	49/74	550.7	1.636 (0.962–2.780)	0.066
Gender				
Female	36/53	587.4	1	
Male	33/59	630.7	0.855 (0.529–1.382)	0.523
Alcohol history[b]				
No	25/43	678.2	1	
Yes	38/61	559.6	1.276 (0.765–2.128)	0.349
History of chronic pancreatitis[c]				
No	47/79	650.9	1	
Yes	7/9	487.4	1.335 (0.600–2.970)	0.478
Tumor size[d]				
≤4	48/80	517	1	
>4	21/30	614.7	1.002 (0.593–1.694)	0.993
Pathologic stage				
I	4/8	528.5	1	
II	65/104	616.4	1.038 (0.375–2.872)	0.943
Neoplasm histologic grade				
G1 + G2	45/80	696.8	1	
G3 + G4	24/32	433.4	2.267 (0.962–5.341)	*0.010*
Targeted molecular therapy[e]				
No	24/29	253.0	1	
Yes	41/73	737.4	1.068 (0.095–0.296)	*<0.001*
Radiation therapy[f]				
No	48/70	561.8	1	
Yes	12/30	705.1	0.527 (0.293–0.947)	*0.029*
Residual resection[g]				
R0	39/66	700.8	1	
R1 + R2	29/44	432.4	1.945 (1.174–3.223)	*0.009*

Italic P values indicate statistically significant. [a], part of data in this table also have been shown in our previous publication; [b], alcohol history is unavailable in 8 patients; [c], history of chronic pancreatitis is unavailable in 24 patients; [d], tumor size is unavailable in 2 patients; [e], targeted molecular therapy information is unavailable in 10 patients; [f], radiation therapy is unavailable in 12 patients; [g], residual resection is unavailable in 10 patients. HR, hazard ratio; MST, mean survival days; OS, overall survival; PDAC, pancreatic ductal adenocarcinoma; HR, hazard ratio; CI, confidence interval.

https://dx.doi.org/10.21037/atm-21-6341

Table S2 The results of prognostic value from low- and high-expression groups of each SLC in PDAC patients' OS

Gene symbol	P value
SLC10A1	0.666
SLC10A2	0.516
SLC10A3	0.032
SLC10A4	0.183
SLC10A5	0.722
SLC10A6	0.766
SLC10A7	0.890
SLC11A1	0.167
SLC11A2	0.522
SLC12A1	0.328
SLC12A2	0.419
SLC12A3	0.216
SLC12A4	0.057
SLC12A5	0.942
SLC12A6	0.135
SLC12A7	0.918
SLC12A8	0.081
SLC12A9	0.615
SLC13A1	0.404
SLC13A2	0.126
SLC13A3	0.464
SLC13A4	0.619
SLC13A5	0.412
SLC14A1	0.722
SLC14A2	0.546
SLC14A2-AS1	0.322
SLC15A1	0.375
SLC15A2	0.553
SLC15A3	0.109
SLC15A4	0.337
SLC16A1	0.996
SLC16A10	0.998
SLC16A11	0.272
SLC16A12	0.959
SLC16A13	0.268
SLC16A14	0.052
SLC16A1-AS1	0.649
SLC16A2	0.131
SLC16A3	0.259
SLC16A4	0.713
SLC16A5	0.466
SLC16A6	0.325
SLC16A6P1	0.933
SLC16A7	0.131
SLC16A8	0.283
SLC16A9	0.794
SLC17A1	0.531
SLC17A2	0.469
SLC17A3	0.939
SLC17A4	0.471
SLC17A5	0.867
SLC17A6	0.468
SLC17A7	0.636
SLC17A8	0.607
SLC17A9	0.704
SLC18A1	0.106
SLC18A2	0.647
SLC18A3	0.868
SLC18B1	0.376
SLC19A1	0.876
SLC19A2	0.303
SLC19A3	0.002
SLC1A1	0.561
SLC1A2	0.733
SLC1A3	0.178
SLC1A4	0.451
SLC1A5	0.994
SLC1A6	0.792
SLC1A7	0.129
SLC22A1	0.584
SLC22A2	0.556
SLC22A1	0.982
SLC22A10	0.425
SLC22A11	0.269
SLC22A13	0.999
SLC22A14	0.016
SLC22A15	0.445
SLC22A16	0.131
SLC22A17	0.100
SLC22A18	0.985
SLC22A18AS	0.631
SLC22A2	0.859
SLC22A20	0.654
SLC22A23	0.001
SLC22A3	0.355
SLC22A31	0.618
SLC22A4	0.027
SLC22A5	0.726
SLC22A7	0.972
SLC22A9	0.747
SLC23A1	0.387
SLC23A2	0.095
SLC23A3	0.694
SLC24A1	0.344
SLC24A2	0.210
SLC24A3	0.059
SLC24A4	<0.001
SLC25A1	0.234
SLC25A10	0.209
SLC25A11	0.036
SLC25A12	0.852
SLC25A13	0.162
SLC25A14	0.504
SLC25A14P1	0.803
SLC25A15	0.959
SLC25A16	0.919
SLC25A17	0.085
SLC25A18	0.375
SLC25A19	0.122
SLC25A1P1	0.240
SLC25A1P5	0.306
SLC25A2	0.751
SLC25A20	0.956
SLC25A21	0.948
SLC25A21-AS1	0.283
SLC25A22	0.018
SLC25A23	0.784
SLC25A24	0.481
SLC25A24P1	0.736
SLC25A25	0.164
SLC25A25-AS1	0.919
SLC25A26	0.184
SLC25A27	0.664
SLC25A28	0.628
SLC25A29	0.744
SLC25A3	0.329
SLC25A30	0.669
SLC25A30-AS1	0.534
SLC25A32	0.078
SLC25A33	0.925
SLC25A34	0.105
SLC25A35	0.504
SLC25A36	0.390
SLC25A36P1	0.126
SLC25A37	0.810
SLC25A38	0.468
SLC25A39	0.010
SLC25A39P1	0.712
SLC25A3P1	0.384
SLC25A4	0.970
SLC25A40	0.602
SLC25A41	0.499
SLC25A42	0.658
SLC25A43	0.188
SLC25A44	0.118
SLC25A45	0.371
SLC25A46	0.363
SLC25A47	0.962
SLC25A48	0.838
SLC25A5	0.188
SLC25A51	0.009
SLC25A52	0.564
SLC25A53	0.112
SLC25A5-AS1	0.053
SLC25A5P1	0.731
SLC25A5P3	0.977
SLC25A5P5	0.480
SLC25A6	0.890
SLC25A6P2	0.836
SLC26A1	0.677
SLC26A10	0.049
SLC26A11	0.740
SLC26A2	0.084
SLC26A3	0.128
SLC26A4	0.758
SLC26A4-AS1	0.547
SLC26A5	0.611
SLC26A6	0.673
SLC26A7	0.656
SLC26A8	0.396
SLC26A9	0.534
SLC27A1	0.926
SLC27A2	0.966
SLC27A3	0.688
SLC27A4	0.086
SLC27A5	0.615
SLC27A6	0.297
SLC28A1	0.955
SLC28A2	0.022
SLC28A3	0.647
SLC29A1	0.623
SLC29A2	0.564
SLC29A3	0.119
SLC29A4	0.811
SLC2A1	0.455
SLC2A10	0.256
SLC2A11	0.847
SLC2A12	0.100
SLC2A13	0.245
SLC2A14	0.161
SLC2A1-AS1	0.781
SLC2A2	0.856
SLC2A3	0.993
SLC2A3P2	0.462
SLC2A3P4	0.244
SLC2A4	0.255
SLC2A4RG	0.382
SLC2A5	0.003
SLC2A6	0.151
SLC2A7	0.356
SLC2A8	0.256
SLC2A9	0.006
SLC30A1	0.539
SLC30A10	0.217
SLC30A2	0.587
SLC30A3	0.319

Table S2 (continued)

Table S2 (continued)

Gene symbol	P value
SLC30A4	0.012
SLC30A5	0.639
SLC30A6	0.810
SLC30A7	0.738
SLC30A8	0.877
SLC30A9	0.068
SLC31A1	0.894
SLC31A1P1	0.873
SLC31A2	0.003
SLC32A1	0.576
SLC33A1	0.550
SLC34A1	0.313
SLC34A2	0.311
SLC34A3	0.279
SLC35A1	0.292
SLC35A2	0.222
SLC35A3	0.457
SLC35A4	0.665
SLC35A5	0.930
SLC35B1	0.372
SLC35B2	0.015
SLC35B3	0.432
SLC35B4	0.029
SLC35C1	0.626
SLC35C2	0.260
SLC35D1	0.304
SLC35D2	0.520
SLC35D3	0.758
SLC35E1	0.979
SLC35E1P1	0.365
SLC35E2	0.030
SLC35E2B	0.741
SLC35E3	0.237
SLC35E4	0.087
SLC35F1	0.396
SLC35F2	0.214
SLC35F3	0.401
SLC35F4	0.715
SLC35F5	0.482
SLC35F6	0.857
SLC35G1	0.823
SLC35G2	0.784
SLC35G5	0.766
SLC35G6	0.880
SLC36A1	0.068
SLC36A2	0.229
SLC36A4	0.803
SLC37A1	0.618
SLC37A2	0.215
SLC37A3	0.827
SLC37A4	0.842
SLC38A1	0.922
SLC38A10	0.890
SLC38A11	0.001
SLC38A2	0.473
SLC38A3	0.408
SLC38A4	0.701
SLC38A5	0.223
SLC38A6	0.461
SLC38A7	0.494
SLC38A8	0.062
SLC38A9	0.441
SLC39A1	0.444
SLC39A10	0.116
SLC39A11	0.030
SLC39A12	0.968
SLC39A13	0.485
SLC39A14	0.698
SLC39A2	0.315
SLC39A3	0.192
SLC39A4	0.289
SLC39A5	0.949
SLC39A6	0.204
SLC39A7	0.712
SLC39A8	0.857
SLC39A9	0.050
SLC3A1	0.520
SLC3A2	0.114
SLC40A1	0.276
SLC41A1	0.375
SLC41A2	0.402
SLC41A3	0.295
SLC43A1	0.513
SLC43A2	0.580
SLC43A3	0.508
SLC44A1	0.921
SLC44A2	0.001
SLC44A3	0.812
SLC44A4	0.789
SLC44A5	0.267
SLC45A1	0.396
SLC45A2	0.230
SLC45A3	0.943
SLC45A4	0.044
SLC46A1	0.674
SLC46A2	0.015
SLC46A3	0.101
SLC47A1	<0.001
SLC47A1P1	0.396
SLC47A2	0.186
SLC48A1	0.141
SLC4A1	0.786
SLC4A10	0.214
SLC4A11	0.033
SLC4A1AP	0.571
SLC4A1APP1	0.808
SLC4A2	0.633
SLC4A3	0.314
SLC4A4	0.798
SLC4A5	0.582
SLC4A7	0.026
SLC4A8	0.088
SLC4A9	0.642
SLC50A1	0.185
SLC51A	0.425
SLC51B	0.517
SLC52A1	0.044
SLC52A2	0.050
SLC52A3	0.201
SLC5A1	0.461
SLC5A10	0.958
SLC5A11	0.541
SLC5A12	0.204
SLC5A2	0.968
SLC5A3	0.569
SLC5A4	0.302
SLC5A5	0.564
SLC5A6	0.362
SLC5A7	0.469
SLC5A8	0.662
SLC5A9	0.972
SLC6A1	0.121
SLC6A11	0.182
SLC6A12	0.977
SLC6A13	0.137
SLC6A14	0.139
SLC6A15	0.594
SLC6A16	0.785
SLC6A17	0.267
SLC6A18	0.121
SLC6A19	0.227
SLC6A1-AS1	0.049
SLC6A2	0.729
SLC6A20	0.366
SLC6A21P	0.315
SLC6A3	0.359
SLC6A4	0.253
SLC6A6	0.151
SLC6A7	0.979
SLC6A8	0.421
SLC6A9	0.978
SLC7A1	0.584
SLC7A10	0.829
SLC7A11	0.663
SLC7A11-AS1	0.221
SLC7A13	0.641
SLC7A14	0.261
SLC7A2	0.238
SLC7A3	0.242
SLC7A4	0.323
SLC7A5	0.118
SLC7A5P1	0.959
SLC7A6	0.138
SLC7A6OS	0.036
SLC7A7	0.492
SLC7A8	0.146
SLC7A9	0.573
SLC8A1	0.055
SLC8A1-AS1	0.736
SLC8A2	0.504
SLC8A3	0.577
SLC8B1	0.468
SLC9A1	0.186
SLC9A2	0.179
SLC9A3	0.071
SLC9A3R1	0.729
SLC9A3R2	0.248
SLC9A4	0.239
SLC9A5	0.370
SLC9A6	0.692
SLC9A7	0.903
SLC9A7P1	0.495
SLC9A8	0.368
SLC9A9	0.248
SLC9B1	0.980
SLC9B2	0.512
SLC9C1	0.734
SLC9C2	0.126
SLCO1A2	0.243
SLCO1B1	0.396
SLCO1B3	0.192
SLCO1B7	0.082
SLCO1C1	0.617
SLCO2A1	0.436
SLCO2B1	0.002
SLCO3A1	0.157
SLCO4A1	0.438
SLCO4A1-AS1	0.759
SLCO4C1	0.076
SLCO5A1	0.020

SLC, solute carrier; PDAC, pancreatic ductal adenocarcinoma; OS, overall survival.

https://dx.doi.org/10.21037/atm-21-6341

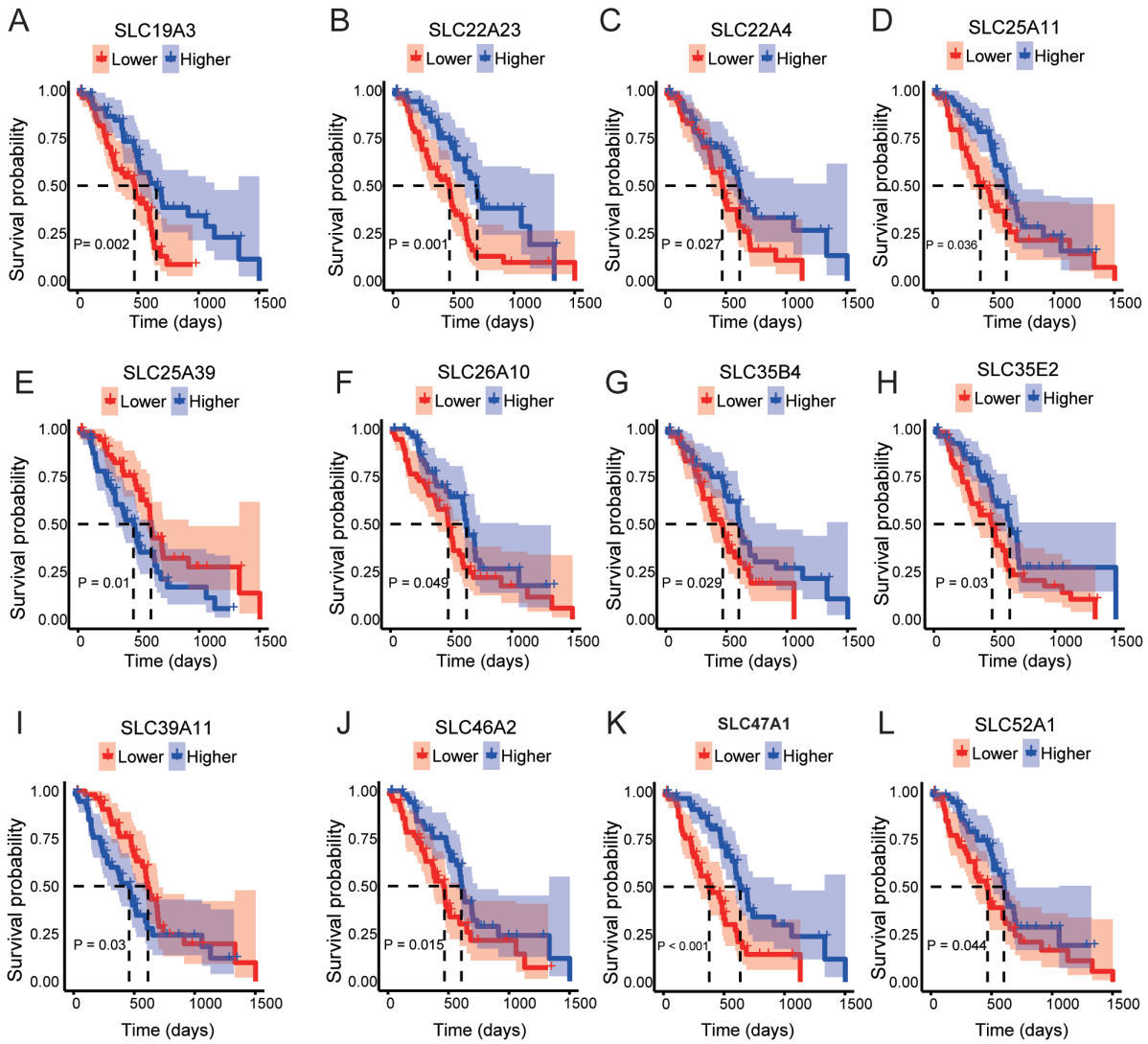

Figure S1 Kaplan-Meier survival curves for SLC genes in PDAC. Overall Survival stratified by (A) *SLC19A3*; (B) *SLC22A23*; (C) *SLC22A4*; (D) *SLC25A11*; (E) *SLC25A39*; (F) *SLC26A10*; (G) *SLC35B4*; (H) *SLC35E2*; (I) *SLC39A11*; (J) *SLC46A2*; (K) *SLC47A1*; (L) *SLC52A1*. SLC, solute carrier; PDAC, pancreatic ductal adenocarcinoma.

https://dx.doi.org/10.21037/atm-21-6341

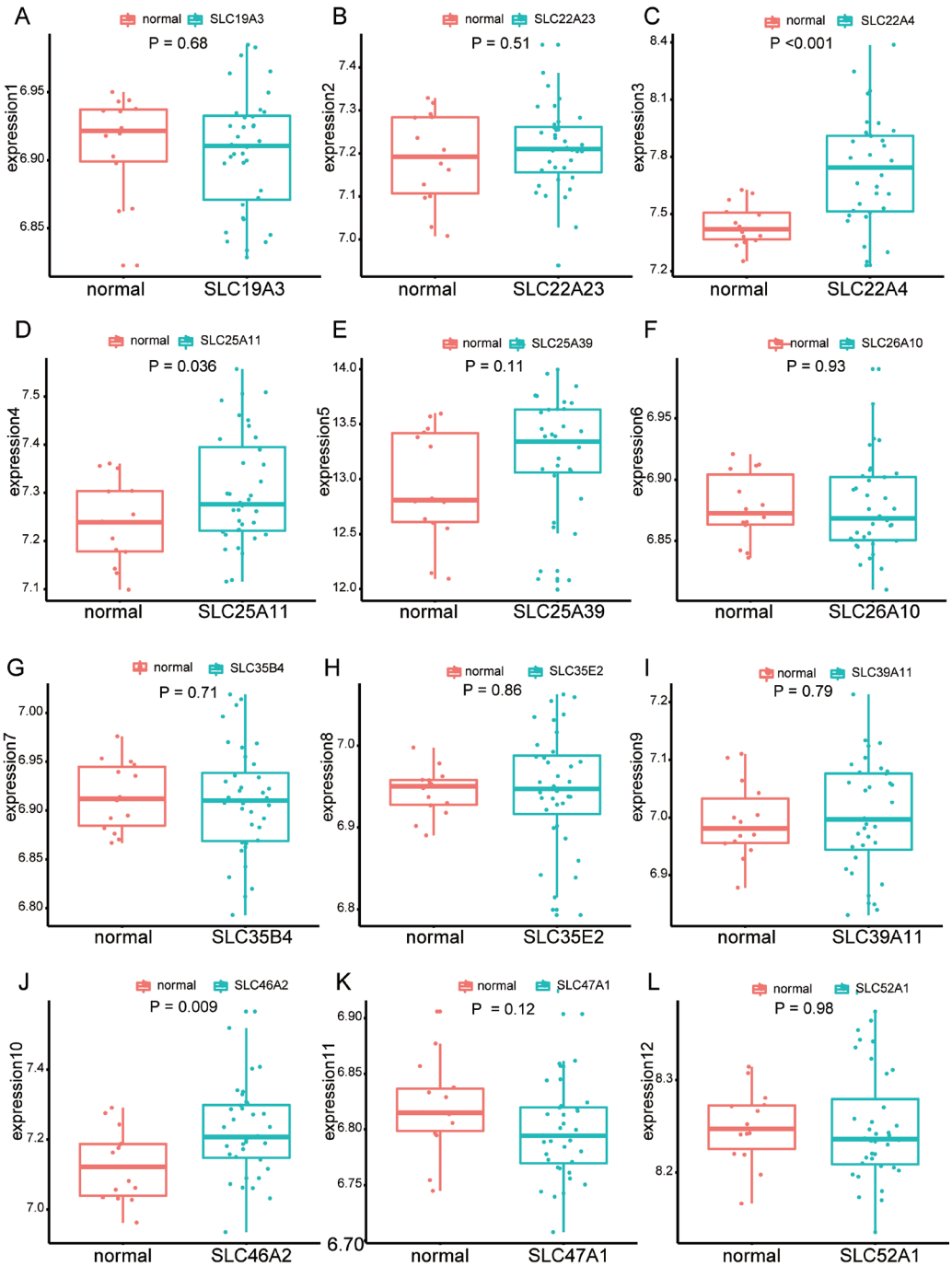

Figure S2 Gene expression level distribution of SLC genes in PDAC peripheral blood and normal peripheral blood of GSE49641. (A) *SLC19A3*; (B) *SLC22A23*; (C) *SLC22A4*; (D) *SLC25A11*; (E) *SLC25A39*; (F) *SLC26A10*; (G) *SLC35B4*; (H) *SLC35E2*; (I) *SLC39A11*; (J) *SLC46A2*; (K) *SLC47A1*; (L) *SLC52A1*. SLC, solute carrier; PDAC, pancreatic ductal adenocarcinoma.

https://dx.doi.org/10.21037/atm-21-6341

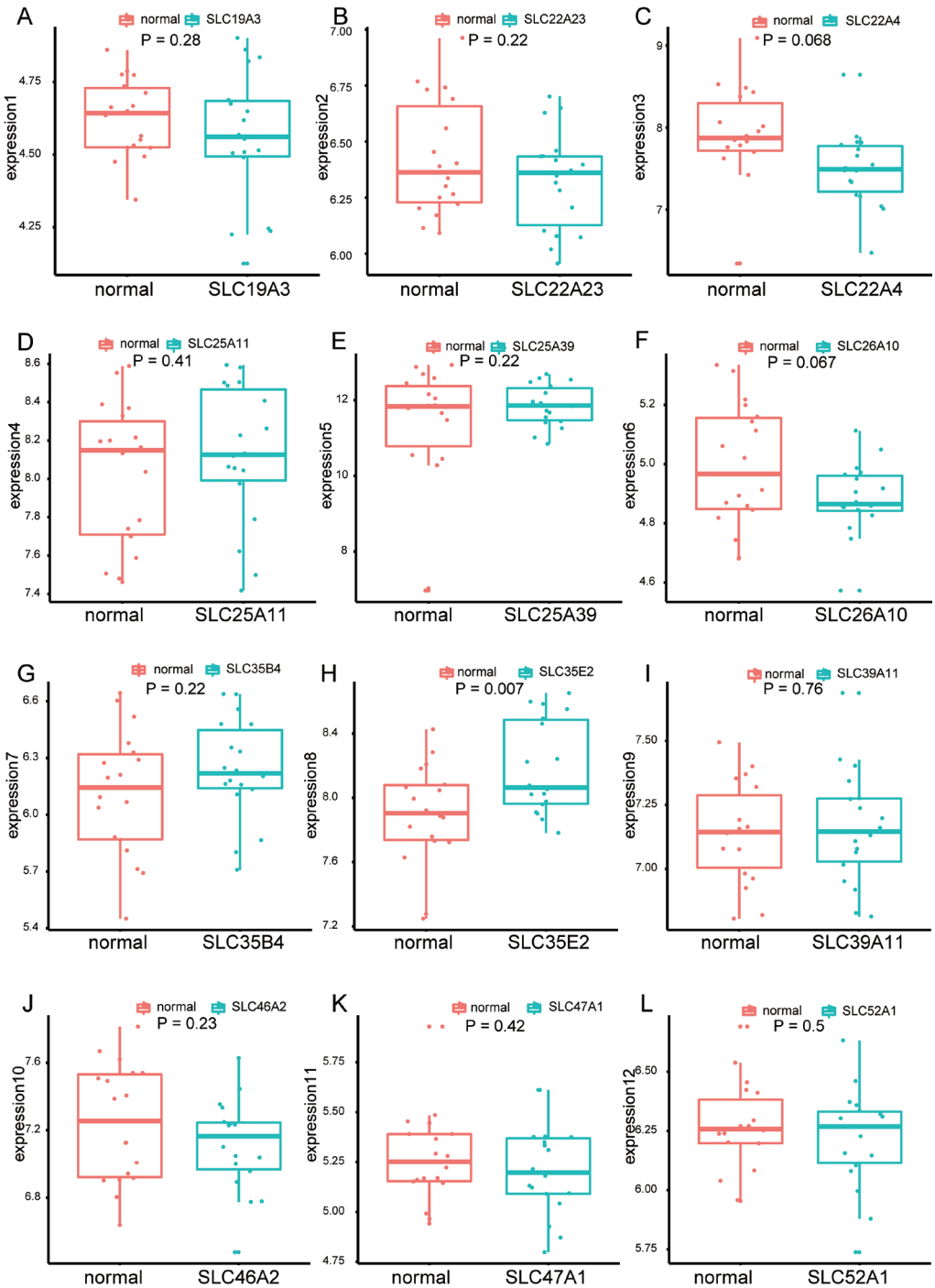

Figure S3 Gene expression level distribution of SLC genes in PDAC peripheral blood and normal peripheral blood of GSE49641. (A) *SLC19A3*; (B) *SLC22A23*; (C) *SLC22A4*; (D) *SLC25A11*; (E) *SLC25A39*; (F) *SLC26A10*; (G) *SLC35B4*; (H) *SLC35E2*; (I) *SLC39A11*; (J) *SLC46A2*; (K) *SLC47A1*; (L) *SLC52A1*. SLC, solute carrier; PDAC, pancreatic ductal adenocarcinoma.

https://dx.doi.org/10.21037/atm-21-6341